Available online at www.sciencedirect.com

SciVerse ScienceDirect

Ceramics International 39 (2013) 6407–6413

CERAMICS INTERNATIONAL

www.elsevier.com/locate/ceramint

Sol–gel auto combustion synthesis of $CoFe_2O_4$/1-methyl-2-pyrrolidone nanocomposite: Its magnetic characterization

U. Kurtan[a,*], R. Topkaya[b], S. Esir[a], A. Baykal[a]

[a]*Department of Chemistry, Fatih University, 34500 B. Çekmece, Istanbul, Turkey*
[b]*Department of Physics, Gebze Institute of Technology, 41400 Gebze-Kocaeli, Turkey*

Received 7 January 2013; received in revised form 22 January 2013; accepted 22 January 2013
Available online 30 January 2013

Abstract

A magnetic nanocomposite was generated by the sol–gel auto-combustion method in the presence of 1-methyl-2-pyrrolidone, a functional solvent. The temperature-dependent magnetic properties of the $CoFe_2O_4$ nanoparticles have been extensively studied in the temperature range of 10–400 K and magnetic fields up to 80 kOe. Zero field cooled (ZFC) and field cooled (FC) curves indicate that the blocking temperature (T_B) of the $CoFe_2O_4$ nanoparticles is above 400 K. It was found from M–H curves that the low temperature saturation magnetization values are higher than bulk value of $CoFe_2O_4$. The saturation magnetization (M_s), remanence magnetization (M_r), reduced remanent magnetization (M_r/M_s) and coercive field (H_c) values decrease with increasing temperature. The M_r/M_s value of 0.75 at 10 K indicates that the $CoFe_2O_4$ nanoparticles used in this work have, as expected, cubic magnetocrystalline anisotropy according to the Stoner–Wohlfarth model. $T^{1/2}$ dependence of the coercive field was observed in the temperature range of 10–400 K according to Kneller's law. The extrapolated T_B and the zero-temperature coercive field values calculated according to Kneller's law are almost 427 K and 13.2 kOe, respectively. The room temperature H_c value is higher than that of the previously reported room temperature bulk values. The effective magnetic anisotropy constant (K_{eff}) was calculated as about 0.23×10^6 erg/cm^3 which is lower than that of the bulk value obtained due to disordered surface spins.

Keywords: 1-Methyl-2-pyrrolidone; $CoFe_2O_4$; Saturation magnetization; Magnetic nanomaterials

1. Introduction

Recently the incorporation of nanoscaled inorganic particles and organic polymers has been widely investigated, considering the extra advantages that could be obtained with combined properties of the inorganic materials (mechanical strength, magnetic and thermal stability) and the organic polymers (flexibility, dielectric, ductility and processibility) [1].

Cobalt ferrite ($CoFe_2O_4$) is one of the most important spinel ferrites with a Curie temperature around 793 K and shows a relatively large magnetic hysteresis. It has wide range of applications including electronic devices, ferrofluids, magnetic delivery microwave devices and high density information storage due to its wealth of magnetic and electronic properties, such as cubic magnetocrystalline anisotropy, high coercivity, moderate saturation magnetization, high Curie temperature TC, photomagnetism, magnetostriction, high chemical stability, wear resistance and electrical insulation, etc. [2–7].

1-Methyl-2-pyrrolidone was chosen as a suitable solvent and a surfactant because it can serve as a coordinating solvent in addition to a high-temperature reaction medium and it is less also less dangerous ac compared with other [8].

Herein, we report a facile hydrothermal method to synthesize $CoFe_2O_4$/1-methyl-2-pyrrolidone nanocomposite with a high yield. Moreover, our products show high saturation magnetization and coercivity at 300 K, which may inspirit more convenient access to the exploration of magnetic materials with special morphology.

*Corresponding author. Tel.: +90 212 866 33 00/2061; fax: +90 212 866 34 02.
E-mail address: ukurtan@fatih.edu.tr (U. Kurtan).

0272-8842/$ - see front matter © 2013 Elsevier Ltd and Techna Group S.r.l. All rights reserved.
http://dx.doi.org/10.1016/j.ceramint.2013.01.067

2. Experimental

2.1. Chemicals and instrumentations

All chemicals including cobalt nitrate tetrahydrate ($Co(NO_3)_2 \cdot 4H_2O$), iron nitrate hexahydrate ($Fe(NO_3)_3 \cdot 6H_2O$), 1-methyl-2-pyrrolidone, ethyl alcohol and acetone were obtained from Merck and used as received, without further purification.

X-ray powder diffraction (XRD) analysis was conducted on a Rigaku Smart Lab Diffractometer operated at 40 kV and 35 mA using Cu K_α radiation.

Scanning Electron Microscopy (SEM) analysis was performed, in order to investigate the microstructure of the sample, using FEI XL40 Sirion FEG Digital Scanning Microscope. Samples were coated with gold at 10 mA for 2 min prior to SEM analysis.

Fourier transform infrared (FT-IR) spectra were recorded in the transmission mode (Perkin Elmer BX FT-IR) on powder samples that were ground with KBr and compressed into a pellet. FT-IR spectra in the range 4000–400 cm^{-1} were recorded in order to investigate the surface characteristics of nanoparticles.

The magnetization measurements were performed by using vibrating sample magnetometer (VSM, Quantum Design, PPMS 9T) in an external field up to 80 kOe in the temperature range of 10–400 K.

2.2. Procedure

Stoichiometric amount of $Fe(NO_3)_3 \cdot 6\,H_2O$ and $Co(NO_3)_2 \cdot 4\,H_2O$ was dissolved in a minimum amount of 1-methyl-2-pyrrolidone and then 25 ml 1-methyl-2-pyrrolidone was added to this solution drop by drop with stirring for 1 h at room temperature. Then, this solution was transferred into an evaporating dish and it is allowed to heat at 190 °C almost for 3 h. During this process, the initial deep red-brown color of the solution changed to a kind of gel. The obtained gel inside evaporating dish was continued to heating and finally brown powders were obtained. After cooled to room temperature, the product was treated with a 3-fold volume excess of ethanol under air to yield a brown precipitate, which could be collected by magnet. The resulting dark brown powder was washed several times with acetone and dried in a vacuum oven at 60 °C overnight (Scheme 1).

3. Results and discussion

3.1. XRD analysis

The X-ray diffraction patterns of the prepared $CoFe_2O_4$ (Fig. 1) shows that the reflection planes ((220), (311), (222), (400), (422), (511) and (440) are indicating the presence of the spinel cubic structure [9]. The mean size of the crystallites was estimated from the diffraction pattern by the line profile fitting method using Eq. (1) given in Refs. [10,11]. The line profile, shown in Fig. 1 was fitted for observed five peaks enlisted above. The average crystallite size was obtained as 23 ± 8 nm as a result of this line profile fitting .

3.2. FT-IR analysis

The FT-IR spectra of $CoFe_2O_4$/1-methyl-2-pyrrolidone nanocomposite and 1-methyl-2-pyrrolidone were given in Fig. 2. Two main broad metal-oxygen bands are seen in the FT-IR spectra of all spinels and ferrites in particular. The highest one, v_1, (Fig. 2a) generally observed in the range 600–550 cm^{-1}, corresponds to intrinsic stretching vibrations of the metal at the tetrahedral site, $M_{tetra} \leftrightarrow O$, whereas the v_2-lowest band, usually observed in the range 450–385 cm^{-1}, is assigned to octahedral–metal stretching, $M_{octa} \leftrightarrow O$ [12]. The FT-IR measurements also reveal that the vibration band C=O shifts from 1680 cm^{-1} for pure 1-methyl-2-pyrrolidone to 1644 cm^{-1} for nanocomposite, which indicates that the O from C=O coordinates with $CoFe_2O_4$ NPs [8]. This observation proves the presence of 1-methyl-2-pyrrolidone on the surface of $CoFe_2O_4$ NPs.

3.3. TG analysis

TG thermograms of $CoFe_2O_4$/1-methyl-2-pyrrolidone nanocomposite were depicted in Fig. 3. TGA measurements were done to determine the relative composition of $CoFe_2O_4$ NPs core, organic shell and solvent residues. Up to 300 °C, there is evaporation of solvent residue and organic shell degradation. After 300 °C, complete evaporation of methyl-2-pyrrolidone was observed $CoFe_2O_4$/1-methyl-2-pyrrolidone nanocomposite has ~5% mass loss for organic shell. Therefore the percentages of organic and inorganic content in the product are 5 and 95 respectively.

3.4. SEM analysis

The morphology of the $CoFe_2O_4$/1-methyl-2-pyrrolidone nanocomposite was determined by scanning electron microscopy (SEM). As shown in Fig. 4, it can be observed that the $CoFe_2O_4$ NPs appear in the uniform sphere-like shape.

3.5. VSM analysis

3.5.1. Dependence of magnetization on temperature

The magnetization curves of the $CoFe_2O_4$ nanoparticles were recorded at different temperatures between 10 and 400 K and in magnetic fields ranging up to 80 kOe (Fig. 5). Inset shows the *M–H* curves of the samples in low field range recorded at 300 and 400 K. The *M–H* curves of the samples exhibit a clear hysteretic behavior at all temperatures, indicates that the $CoFe_2O_4$ nanoparticles prepared by the sol–gel auto-combustion method in this study have ferromagnetic behavior at all temperatures between 10 and 400 K. This character makes the $CoFe_2O_4$ nanoparticles prepared by the sol–gel auto-combustion method in this work a potential candidate

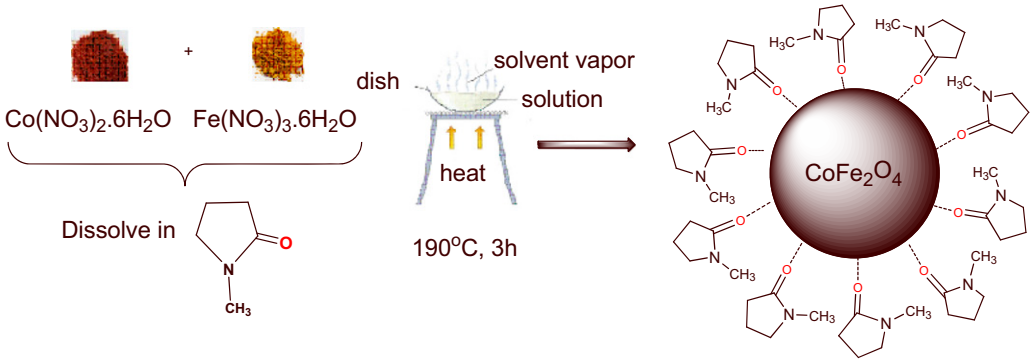

Scheme 1. Synthesis of $CoFe_2O_4$/1-methyl-2-pyrrolidone nanocomposite.

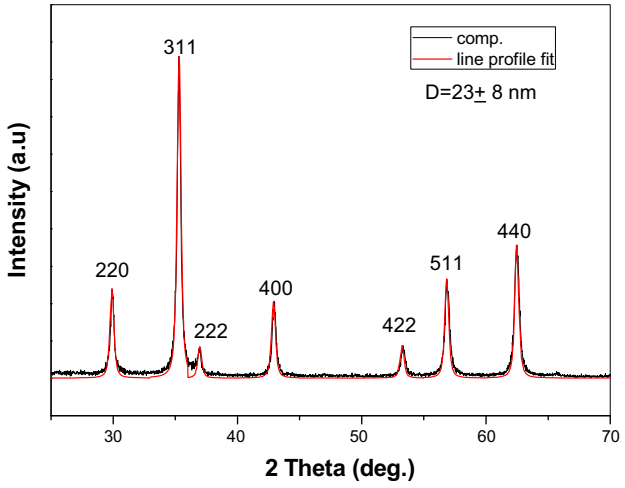

Fig.1. XRD powder pattern of $CoFe_2O_4$/1-methyl-2-pyrrolidone nanocomposite.

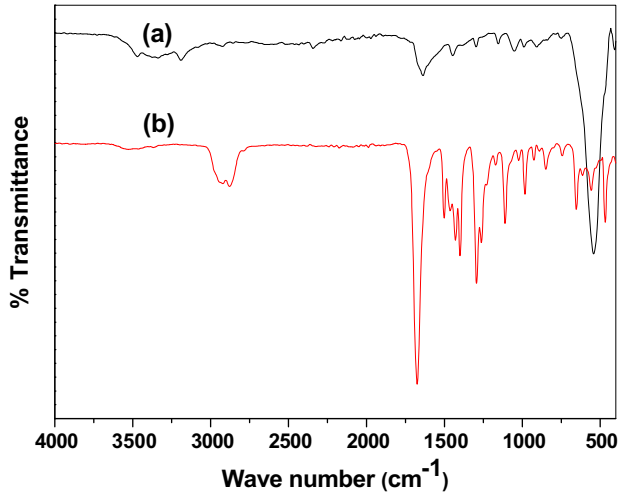

Fig.2. FT-IR spectra of (a) $CoFe_2O_4$/1-methyl-2-pyrrolidone nanocomposite and (b) 1-methyl-2-pyrrolidone.

for the applications in magnetic recording technology. The observed hysteretic behavior at 400 K exhibits that the blocking temperature (T_B) for superparamagnetic particles in the samples is above 400 K. It can be easily seen from hysteresis loops that magnetization does not completely saturate, suggesting the existence of antiferromagnetic interactions [13,14]. In the literature, similar results have been reported in the $Mn_{0.2}Ni_{0.8}Fe_2O_4$ nanoparticles synthesized by a PEG-assisted hydrothermal route [15] and triethylene glycol coated $Mn_xCo_{1-x}Fe_2O_4$ nanoparticles prepared by the glycothermal reaction [14]. The ferromagnetic contribution saturates the magnetization, while as the antiferromagnetic contribution linearly enhances it, resulting in nonsaturated magnetization behavior [13].

Dependence of the saturation magnetization (M_s) of the $CoFe_2O_4$ nanoparticles on temperature is shown in Fig. 6. The M_s values of the $CoFe_2O_4$ nanoparticles at different temperatures were determined by extrapolating the M vs. $1/H$ plot to $1/H=0$. It can be seen that M_s continuously increases with decreasing the temperature from 400 to 50 K and later decreases from 50 to 10 K. In a spinel structure, the magnetic moments in the octahedral (B) and tetrahedral (A) sites are coupled antiparallel to each other. Thus, total magnetic moment is $M_{oct}-M_{tet}$ where M_{oct} and M_{tet} are the B and A sublattice magnetic moments, respectively. Dependence of the magnetic moments in the octahedral (B) and tetrahedral (A) sites on temperature can be different from each other [16]. Therefore, with increasing temperature, firstly, M_s increases and later decreases. Similar behavior has been reported in Bi-substituted cobalt ferrite nanoparticles synthesized by a combustion reaction method [17] and the $CoFe_2O_4$ nanoparticles synthesized by a combustion reaction method [18]. Also, low temperature saturation magnetization values are higher than that of the bulk cobalt ferrite (80 emu/g) [16]. The higher M_s values than that of the bulk value can be ascribed to the magnetic interactions tending to enhance the M_s [19].

3.5.2. *Variation of remanence magnetization with temperature*

Fig. 7 represents thermal dependence of the remanence magnetization, M_r for the $CoFe_2O_4$ nanoparticles. The inset in Fig. 7 shows the change of the reduced remanent magnetization (M_r/M_s) with temperature. It is clear that the M_r and M_r/M_s increases with decreasing temperature. For non-interacting mono domain particles with the randomly oriented

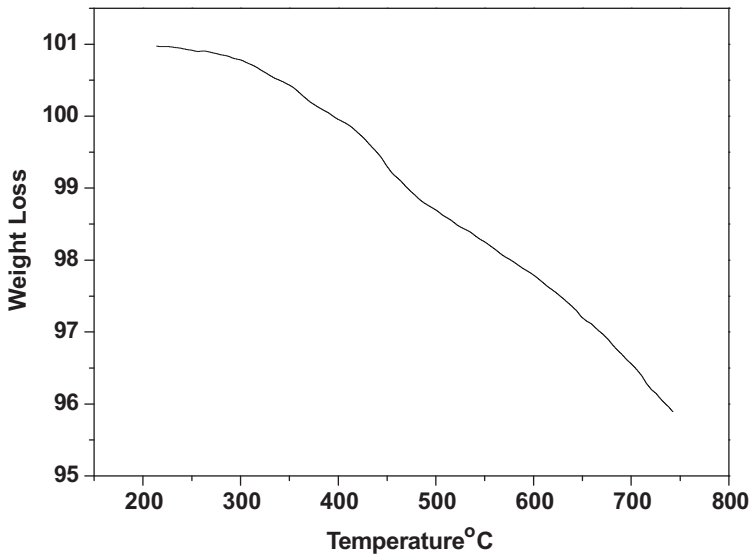

Fig.3. TG thermogram of $CoFe_2O_4$/1-methyl-2-pyrrolidone nanocomposite.

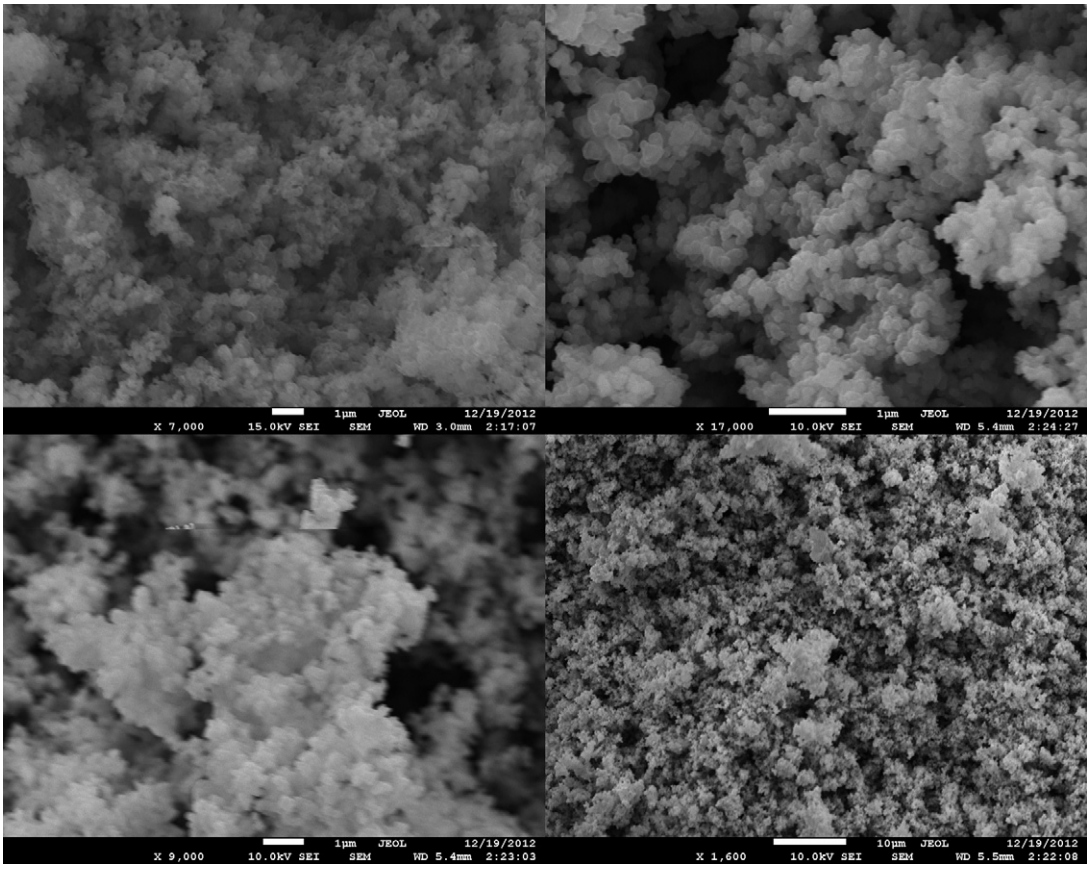

Fig. 4. SEM micrographas of $CoFe_2O_4$/1-methyl-2-pyrrolidone nanocomposite with different magnfications.

easy axis, the M_r/M_s is given as 0.5 for uniaxial anisotropy, and 0.832 for cubic anisotropy in the Stoner–Wohlfarth model [20]. As can be seen from the inset of Fig. 7, the M_r/M_s value of the $CoFe_2O_4$ nanoparticles used in this study is 0.75 at 10 K. Taking into account that bulk $CoFe_2O_4$ a well known ferrimagnetic material with high cubic magnetocrystalline anisotropy [16], it can be concluded that the $CoFe_2O_4$ nanoparticles prepared by the sol–gel auto-combustion method in this study have cubic magnetocrystalline anisotropy. Similar results have been reported in nearly monodispersed $CoFe_2O_4$ nanoparticles by Chinnasamy et al. [21] and single domain $CoFe_2O_4$ nanoparticles by Pal et al. [22].

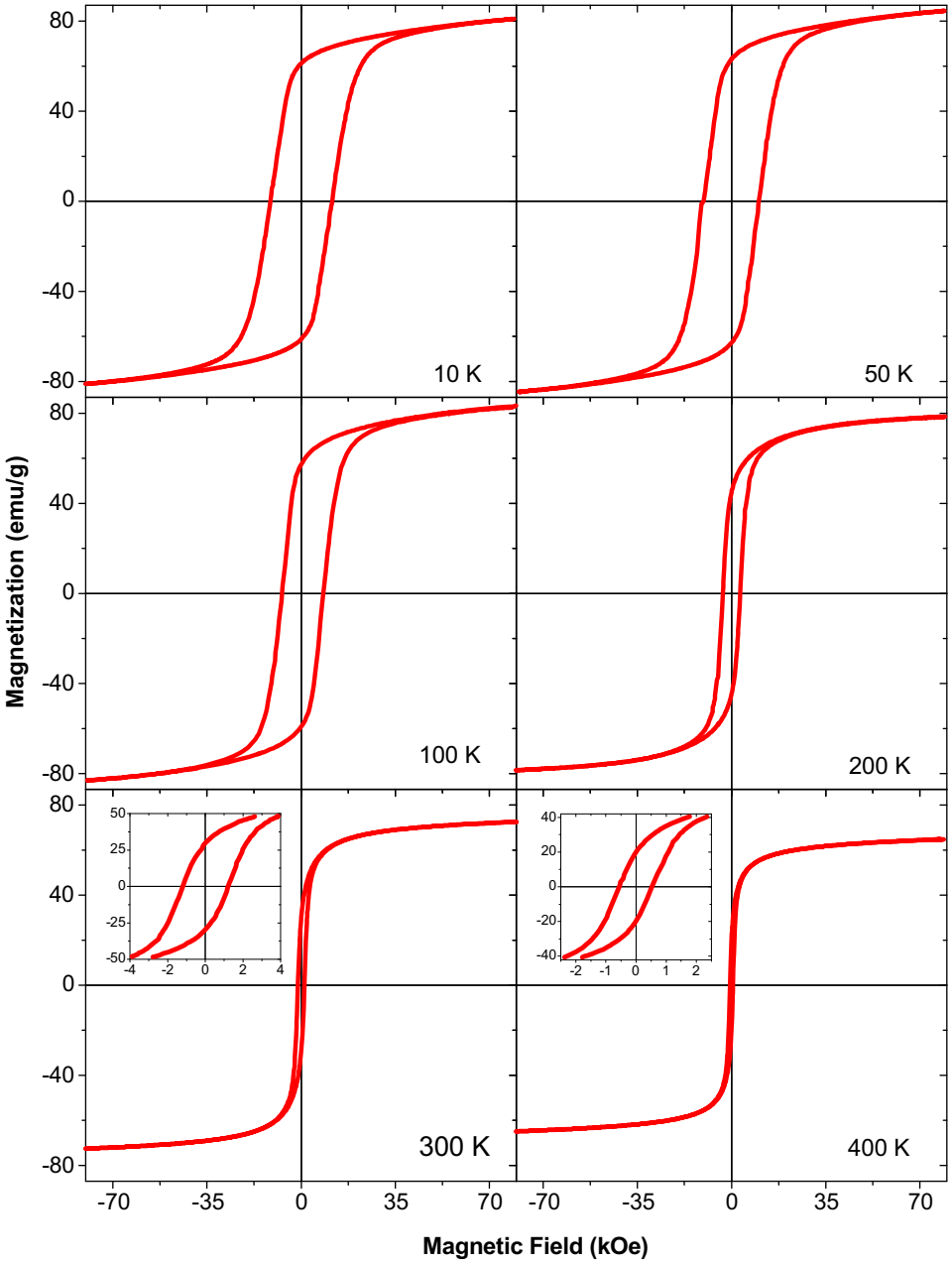

Fig. 5. The variation of magnetization with the applied magnetic field recorded at different temperatures for $CoFe_2O_4$/1-methyl-2-pyrrolidone nanocomposite. Inset shows the hysteresis loops in low field range recorded at 300 and 400 K.

3.5.3. Linear coercive field behavior

When the coercive field (H_c) values are plotted with square root of the temperature (Fig. 8), almost linear behavior was observed. The linear behavior of the H_c follows the equation (Kneller's law):

$$H_C(T) = H_{C_0}\left[1-\left(\frac{T}{T_B}\right)^{1/2}\right] \quad (1)$$

where H_{c_0} is the coercive field at $T=0$ K and T_B is the mean value of the superparamagnetic blocking temperature. The T_B and H_{c_0} values determined from the fit according to the Kneller's relation are almost 427 K and 13.2 kOe, respectively. At the blocking temperature, the energy barrier E_B, is comparable to the thermal energy, k_BT and the spins randomly fluctuate. This phenomenon is termed as superparamagnetism [23]. Moreover, as seen from fig. 8, the H_c values continuously increases with decreasing temperature. When the temperature decreases, the quantity of Co^{2+} ions in the octahedral (B) sites increase, resulting in increase of the effective magnetic anisotropy [24]. In this study, as the temperature decreases, the H_c increases due to the increasing effective magnetic anisotropy constant K_{eff} according to the relation $H_c=2K_{eff}/M_s$.

In this study, the H_c values of the $CoFe_2O_4$ nanoparticles are 1202 and 545 Oe at 300 and 400 K, respectively. The room temperature coercive field value is higher than that of the bulk

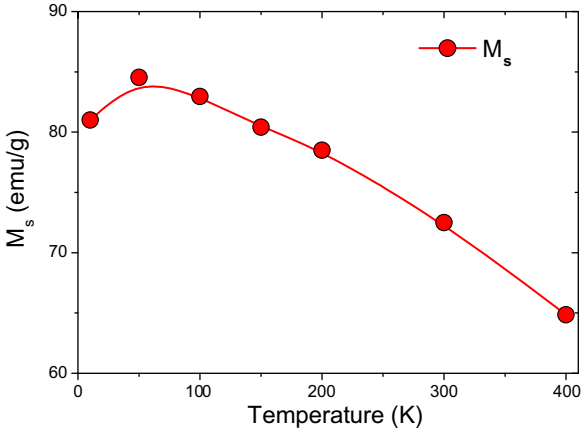

Fig. 6. Thermal dependence of saturation magnetization (M_s) of the $CoFe_2O_4$/1-methyl-2-pyrrolidone nanocomposite.

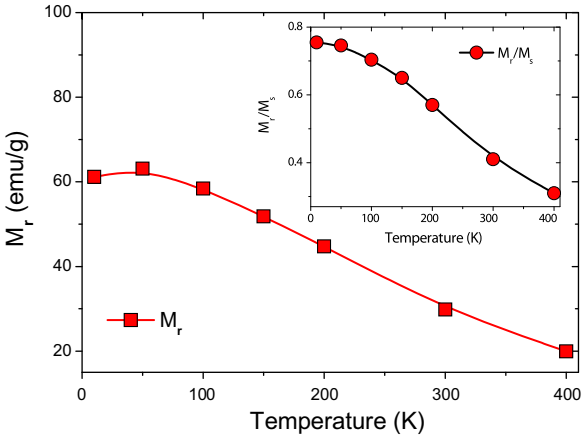

Fig. 7. Variation of the remanence magnetization, M_r for the $CoFe_2O_4$/1-methyl-2-pyrrolidone nanocomposite with temperature. Inset: the variation of the reduced remanent magnetization (M_r/M_s) with temperature.

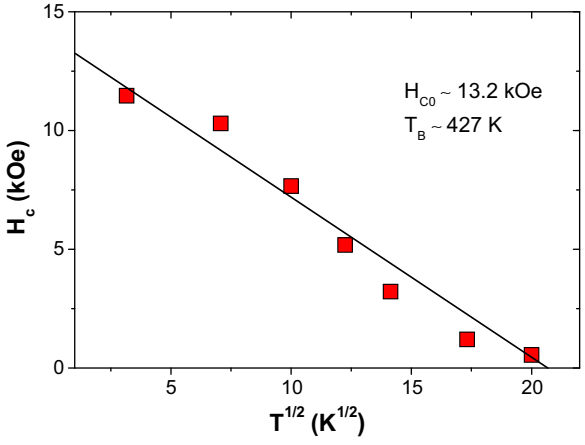

Fig. 8. Thermal dependence of coercive field (H_c) of the $CoFe_2O_4$/1-methyl-2-pyrrolidone nanocomposite articles below T_B. The curve shows the linear fit to the experimental data according to Kneller's law.

$CoFe_2O_4$ [25]. In literature, at room temperature the coercivity values higher than that of the bulk value have been reported in cobalt ferrite particles by Sangmanee and Maensiri [26] and Jeppson et al. [27]. The higher H_c values of the $CoFe_2O_4$ nanoparticles used in this study can be appropriate for the applications that require higher temperatures than room temperature. In general, the effective magnetic anisotropy constant, K_{eff} of the magnetic nanoparticles is determined by using the following relation [28]:

$$K_{eff} V = 25 k_B T_B \quad (2)$$

where V, k_B, T_B are the volume of a single particle, Boltzmann constant, and blocking temperature, respectively. In this study, the calculated effective magnetic anisotropy constant, K_{eff} for the $CoFe_2O_4$ nanoparticles is about 0.23×10^6 erg/cm^3. This value is lower than that of the bulk $CoFe_2O_4$ [16]. The possible reason can be the disordered surface spins of the $CoFe_2O_4$ nanoparticles [29].

4. Conclusion

First, the facile synthetic method allows highly crystalline and monodisperse nanoparticles. The average crystallite size of $CoFe_2O_4$/1-methyl-2-pyrrolidone nanocomposite was obtained as 23 ± 8 nm as a result of this line profile fitting. FT-IR proved the bonding between $CoFe_2O_4$ NPs and 1-methyl-2-pyrrolidone via C=O. ZFC and FC curves indicate that the T_B of the $CoFe_2O_4$/1-methyl-2-pyrrolidone nanocomposite is above 400 K. It was observed from M–H curves that the M_s, K_{eff}, H_c, M_r, and M_r/M_s strongly depend on temperature. The low temperature M_s values are found to be higher than that of the bulk $CoFe_2O_4$. According to the Stoner–Wohlfarth model, the M_r/M_s value of 0.75 at 10 K indicates that the $CoFe_2O_4$ nanoparticles used in this work have cubic magnetocrystalline anisotropy as expected. From the linear dependence of H_c on the square root of the temperature, T_B and the zero-temperature coercive field values are determined as ~427 K and 13.2 kOe, respectively. The effective magnetic anisotropy constant (K_{eff}) was calculated as about 0.23×10^6 erg/cm^3.

Acknowledgments

This work is supported by Fatih University under BAP Grant no. P50021104-B.

References

[1] H. Liu, F. Xu, L. Li, Y. Wang, H. Qiu, A novel $CoFe_2O_4$/polyacrylate nanocomposite prepared via an in situ polymerization in emulsion system, Reactive and Functional Polymers 69 (2009) 43–47.
[2] R.V. Chopdekar, Y. Suzuki, Magnetoelectric coupling in epitaxial $CoFe_2O_4$ on $BaTiO_3$, Applied Physics Letters 89 (2006) 182506–182510.
[3] H. Zheng, F. Straub, Q. Zhan, P.-L. Yang, W.-K. Hsieh, F. Zavaliche, Y.-H. Chu, U. Dahmen, R. Ramesh, Self-assembled growth of $BiFeO_3$–$CoFe_2O_4$ nanostructures, Advanced Materials 18 (2006) 2747–2752.
[4] T.M. Whitney, J.S. Jiang, P.C. Searson, C. Chien, Fabrication and magnetic properties of arrays of metallic nanowires, Science 261 (1993) 1316–1319.
[5] I.H. Gul, A.Z. Abbasi, F. Amin, M. Anis-ur-Rehman, A. Maqsood, Structural, magnetic and electrical properties of $Co_{1-x}Zn_xFe_2O_4$

synthesized by the co-precipitation method, Journal of Magnetism and Magnetic Materials 311 (2007) 494–499.
[6] J.J. Versluijs, M.A. Bari, J.M.D. Coey, Magnetoresistance of half-metallic oxid nanocontacts, Physical Review Letters 87 (2001) 026601–026604.
[7] S. Kazan, Magnetic properties of triethylene glycol coated $CoFe_2O_4$ and $Mn_{0.2}Co_{0.8}Fe_2O_4$ NP's synthesized by the polyol method, Arabian Journal of Chemistry (2012), http://dx.doi.org/10.1016/j.arabjc.2011.12.005.
[8] C. Qin, C. Li, Y. Hu, J. Shen, M. Ye, Facile synthesis of magnetic iron oxide nanoparticles using 1-methyl-2-pyrrolidone as a functional solvent, Colloids and Surfaces A: Physicochemical and Engineering Aspects 336 (2009) 130–134.
[9] N. Kasapoğlu, A. Baykal, Y. Köseoğlu, M.S. Toprak, Microwave-assisted combustion synthesis of $CoFe_2O_4$ with urea and its magnetic characterization, Scripta Materialia 57 (2007) 441–444.
[10] T. Wejrzanowski, R. Pielaszek, A. Opalinska, H. Matysiak, W. Łojkowski, K.J. Kurzydłowski, Applied Surface Science 253 (2006) 204–209.
[11 R. Pielaszek, Analytical expression for diffraction line profile for polydispersive powders, applied crystallography in: Proceedings of the XIX Conference, Krakow, Poland; 2003, p. 43.
[12] R.D. Waldron, Infrared spectra of ferrites, Physical Review 99 (1955) 1727.
[13] K.K. Bharathi, R.J. Tackett, C.E. Botez, C.V. Ramana, Coexistence of spin glass behavior and long-range ferrimagnetic ordering in La- and Dy-doped Co ferrite, Journal of Applied Physics 109 (2011) 07A510.
[14] R. Topkaya, Ö. Akman, S. Kazan, B. Aktaş, Z. Durmus, A. Baykal, Surface spin disorder and spin-glass-like behavior in manganese-substituted cobalt ferrite nanoparticles, Journal of Nanoparticle Research 14 (2012) 1156.
[15] Y. Köseoğlu, M. Bay, M. Tan, A. Baykal, H. Sözeri, R. Topkaya, N. Akdoğan, Magnetic and dielectric properties of $Mn_{0.2}Ni_{0.8}Fe_2O_4$ nanoparticles synthesized by PEG-assisted hydrothermal method, Journal of Nanoparticle Research 13 (2011) 2235–2244.
[16] B.D. Cullity, C.D. Graham, Introduction to Magnetic Materials, 2nd ed., Addison-Wesley, New Jersey, 2009, pp. 187–188.
[17] A. Franco Jr., F.L.A. Machado, V.S. Zapf, F. Wolff-Fabris, Journal of Applied Physics 109 (2011) 07A745.
[18] A. Franco, F.L.A. Machado, V.S. Zapf, Journal of Applied Physics 110 (2011) 053913.
[19] P. Jeppson, R. Sailer, E. Jarabek, J. Sandstrom, B. Anderson, M. Bremer, D.G. Grier, D.L. Schulz, A.N. Caruso, Journal of Applied Physics 100 (2006) 114324.
[20] E.C. Stoner, E.P. Wohlfarth, A mechanism of magnetic hysteresis in heterogeneous alloys, Philosophical Transactions of the Royal Society of London A 240 (826) (1948) 599–642, http://dx.doi.org/10.1098/rsta.1948.0007.
[21] C.N. Chinnasamy, B. Jeyadevan, K. Shinoda, K. Tohji, D.I. Djayaprawira, M. Takahashi, R.J. Joseyphus, A. Narayanasamy, Unusually high coercivity and critical single-domain size of nearly monodispersed $CoFe_2O_4$ nanoparticles, Applied Physics Letters 83 (2003) 2862.
[22] D. Pal, M. Mandal, A. Chaudhuri, B. Das, D. Sarkar, K. Mandal, Micelles induced high coercivity in single domain cobalt ferrite nanoparticles, Journal of Applied Physics 108 (2010) 124317.
[23] A. Herpin, Theorie du Magnetism, 1st ed., Institut National des Sciences et Techniques Nucle´aires¸ Paris¸ 1968¨
[24] M. Tachiki, Origin of the magnetic anisotropy energy of cobalt ferrite, Progress of Theoritical Physics 23 (1055) (1960) 1055–1072, http://dx.doi.org/10.1143/PTP.23.1055.
[25] D.J. Craik, Magnetic Oxides, part 2, John Wiley & Sons, London, 1975, pp. 703.
[26] M. Sangmanee, S. Maensiri, Nanostructures and magnetic properties of cobalt ferrite ($CoFe_2O_4$) fabricated by electrospinning, Applied Physics A 97 (2009) 167–177.
[27] P. Jeppson, R. Sailer, E. Jarabek, J. Sandstrom, B. Anderson, M. Bremer, D.G. Grier, D.L. Schulz, A.N. Caruso, Journal of Applied Physics 100 (2006) 114324.
[28] T. Hyeon, Y. Chung, J. Park, S.S. Lee, Y.W. Kim, B.H. Park, Synthesis of highly crystalline and monodisperse cobalt ferrite nanocrystals, Journal of Physical Chemistry B 106 (2002) 6831.
[29] R.D. Desautels, J.M. Cadogan, J.V. Lierop, Spin dynamics in $CoFe_2O_4$ nanoparticles, Journal of Applied Physics 105 (2009) 07B506.